

PERPETUAL PAVEMENT EVALUATION USING THE VISCOELASTIC CONTINUUM DAMAGE FINITE ELEMENT PROGRAM

Y. Richard Kim, Ph.D., P.E.

Professor

Dept. of Civil, Construction, & Environmental Engineering

Campus Box 7908

North Carolina State University

Raleigh, North Carolina 27695-7908

Ph: (919) 515-7758

Fax: (919) 515-7908

Email: kim@ncsu.edu

Shane Underwood

Graduate Research Assistant

Dept. of Civil, Construction, & Environmental Engineering

North Carolina State University

Sungho Mun, Ph.D.

Senior Researcher

Pavement Research Group

Highway & Transportation Technology Institute

Korea Highway Corporation

50-5 Sancheok-ri Dongtan-myeon Hwaseong-si

Kyonggi-do, South Korea

Ph: 82-31-371-3360

Fax: 82-31-371-3369

Email: smun@freeway.co.kr

Murthy N. Guddati, Ph.D.

Associate Professor

Dept. of Civil, Construction, & Environmental Engineering

Campus Box 7908

North Carolina State University

Raleigh, North Carolina 27695-7908

Ph: (919) 515-7699

Fax: (919) 515-7908

Email: mnguddat@eos.ncsu.edu

Word Count: $4927+10(250) = 7427$ (2 Tables, 8 Figures)

Submitted to the International Conference on Perpetual Pavement

August 2006

ABSTRACT

This paper presents the experimental/analytical/computational research at North Carolina State University that has as its objective the development of a mechanistic pavement performance modeling methodology for asphalt pavements. The material model used for hot mix asphalt (HMA) mixtures is the viscoelastoplastic continuum damage (VEPCD) model. The VEPCD model is used to evaluate the performance of four HMA mixtures constructed at the Federal Highway Administration's Accelerated Loading Facility (FHWA ALF). Polymer-modified asphalt binders are used with three of the four asphalt mixtures investigated in this study.

Cracking performance of pavements with different HMA layer thicknesses and layer material strengths is evaluated using the viscoelastic continuum damage (VECD) model implemented in the public domain finite element program, FEP++. Both bottom-up and top-down cracks are investigated by taking several important variables into account, such as asphalt layer thickness, layer stiffness, pressure distribution under loading, and load level applied on the pavement surface. The cracking mechanisms in various pavement structures under different loading conditions are studied by monitoring a damage contour. Preferred conditions for top-down cracking have been identified using the results from this parametric study. The conjoined damage contours in thicker pavements suggest that the through-the-thickness crack may develop as the bottom-up and top-down cracks propagate simultaneously and coalesce together, supporting observations made from field cores and raising the question of the validity of traditional fatigue performance models that account for the growth of bottom-up cracking only.

The flexible nature of the VECD-FEP++ modeling technique allows cracks to initiate and propagate wherever the fundamental material law suggests and, therefore, it is not necessary to assume *a priori* the location of distress initiation nor the path of distress evolution. As a result, a much more realistic and accurate cracking simulation in perpetual pavements can be accomplished using the VECD-FEP++.

Key Words: asphalt, viscoelasticity, viscoplasticity, continuum damage, polymer-modified, ALF, VECD, VEPCD, FEP++, top-down cracking, perpetual pavements

INTRODUCTION

A perpetual pavement concept has been considered as one of the options to help increase pavement life. Perpetual pavements are designed to resist bottom-up cracking by incorporating thick hot mix asphalt (HMA) layers that limit the tensile strain at the bottom of the HMA layer so that the tensile strain is below the endurance limit. In addition, their design resists bottom-up cracking by using a binder-rich HMA mixture at the bottom of the HMA layers. Typically, rutting is minimized by using rut-resistant HMA mixtures in the top three to four inches. The successful application of this design concept results in an asphalt pavement that requires only routine maintenance that involves replacing the surface course periodically without the need for repairing deeper layers.

However, the perpetual pavement concept based on limiting tensile strain at the bottom of HMA layers does not consider cracks that start from the pavement surface and propagate downward, i.e., top-down cracking. Many field studies have proven that top-down cracking is the major cracking mechanism in thick asphalt pavements. Different patterns of top-down cracking are reported from these field studies, including cracks that start from the pavement surface and propagate downward, cracks that start as a top-down crack and propagate horizontally at the layer interface, and cracks that start from both the top and bottom simultaneously, forming a conjoined cracking pattern. Complex combinations of layer material types and thicknesses in perpetual pavements make it more difficult to predict the failure mechanisms using conventional HMA performance prediction models and pavement response models.

With the goal of accurate pavement performance evaluation, the researchers at North Carolina State University (NCSU) have been developing advanced models for HMA under complex loading conditions. Over the past decade, they have been successful in developing material models that can accurately capture various critical phenomena, such as: microcrack-induced damage, which is critical for fatigue modeling; strain rate-temperature interdependence; and viscoplastic flow, which is critical for high temperature modeling. The resulting model is termed the viscoelastoplastic continuum damage (VEPCD) model.

To extend the strengths of the VEPCD model to fatigue cracking evaluation of pavement systems, the viscoelastic continuum damage (VECD) model has been incorporated into the public domain finite element code, FEP++. The resulting product, the so-called VECD-FEP++, allows the accurate evaluation of boundary condition effects (e.g., layer thicknesses) on the material behavior. Currently, the NCSU researchers are working to include the full VEPCD model into the FEP++. In the VECD-FEP++, the damage is calculated for each element based on its state of stress, temperature, loading rate, and boundary conditions. Therefore, it is not necessary to assume *a priori* the location of distress initiation, nor the path of distress evolution. Not having to make such assumptions is a feature of the VECD-FEP++ that is essential in evaluating complex pavement structures in perpetual pavements. The flexible nature of the VECD-FEP++ modeling technique allows cracks to initiate and propagate wherever the fundamental material law suggests. As a result, much more realistic and accurate cracking simulation can be accomplished using the VECD-FEP++.

This paper introduces the VECD-FEP++ as a means of designing and evaluating perpetual pavements. First, the VEPCD model and its application to modified HMA mixtures used in the Federal Highway Administration (FHWA) Accelerated Loading Facility (ALF) are discussed. Then, the results from the VECD-FEP++ simulations on pavements with different HMA layer thicknesses and loading conditions are presented.

MATERIAL MODEL

Viscoelastic Continuum Damage (VECD) Model

Kim et al. (2) developed a uniaxial viscoelastic continuum damage model by applying the elastic-viscoelastic correspondence principle, based on pseudo strain, to separate the effects of viscoelasticity and damage. In the authors' approach, an internal state variable is formulated based on the work potential theory to account for the damage evolution under cyclic loading and the microdamage healing during rest periods. From the verification study, it was found that the constitutive model accurately predicts the stress-strain behavior of asphalt concrete under varying loading rates, random rest durations, multiple stress/strain levels, and different modes of loading (controlled-stress versus controlled-strain). Continuing efforts show that a unique relationship exists between the internal state variable (S) and the normalized pseudo stiffness (C), regardless of the applied loading conditions (cyclic versus monotonic, amplitude/rate, and frequency) (3). This characteristic curve describes the reduction in material integrity (C) as damage (S) grows in the asphalt concrete specimen. Still further work demonstrates that asphalt concrete remains thermorheologically simple at high tensile damage levels (4). These findings simultaneously simplify characterization by allowing for the prediction of mixture responses at various temperatures from laboratory testing at a single temperature. The damage characteristic curve and the time-temperature superposition principle with growing damage are the foundations of the VECD model employed in this study.

Viscoplastic (VP) Model

Although the current VECD-FEP++ formulation does not include viscoplasticity, a brief introduction to this concept is given here. The VECD model, outlined above, is applicable only to conditions where viscoelastic damage mechanisms dominate the material behavior. However, it is known that, in the field, other mechanisms, particularly viscoplasticity, influence the material performance. Considering this fact, researchers of the NCHRP 9-19 project deemed it necessary to combine the VECD model with some other model so that the viscoplastic effects would be taken into account (4). The model developed by these researchers is based on Uzan's work with strain hardening and viscoplasticity (23) and was implemented based on the strain decomposition principle outlined by Schapery (22).

Universal Model

One of the most widely accepted constitutive models for unbound materials is the universal model (7) shown below:

$$M_r = k_1 P_a \left(\frac{\theta}{P_a} \right)^{k_2} \left(\frac{\sigma_d}{P_a} \right)^{k_3}, \quad (1)$$

where k_1 to k_3 are regression constants, P_a is atmospheric pressure, θ is bulk stress, and σ_d is deviator stress. This model describes the nonlinear stress-strain characteristics of cohesive and granular soils by expressing the resilient modulus as a function of the stress state. The finite element methods of the nonlinear elastic models have been implemented using iterative search techniques (8, 9). The current numerical implementation is based on the more efficient Newton-type method suggested by Hjelmstad et al. (10). These researchers recast the stress-dependent

resilient modulus into the strain-dependent modulus by relating stress invariants to strain invariants. The resulting model is amenable to implementation in a standard displacement-based finite element framework. The finite element program with the universal model was verified using analytical solutions of simple boundary condition problems (6).

VEPCD MODELING OF FHWA-ALF MIXTURES

Materials and Specimen Fabrication

As part of the continuing development of the VEPCD model, an experimental study has been undertaken wherein mixtures tested beneath the Federal Highway Administration's Accelerated Loading Facility (FHWA ALF) have been characterized within the VEPCD framework. The aggregate structure for each of the mixtures was the same, Superpave 12.5mm coarse. Four asphalt binders, one unmodified (Control-PG 70-22) and three polymer-modified (Crumb Rubber Terminal Blend-PG 76-28, Styrene-Butadiene-Styrene-PG 70-28 and Ethylene Terpolymer-PG 70-28), of similar performance grading were used for this study. The asphalt content for each mixture was set at 5.3% by total mix mass. Further details of the mixtures used in this study, along with specimen fabrication information, are presented elsewhere (21, 9, 17).

Characterization

Full characterization of the VEPCD model is accomplished through a three-step process. The first step is to assess the linear viscoelastic properties of the material using dynamic modulus, or temperature/frequency sweep, testing. This test method is given in AASHTO TP-62 and is one of the proposed Superpave simple performance tests. The second step is the viscoelastic continuum damage (VECD) characterization, which is accomplished using constant crosshead rate tests under conditions where such mechanisms dominate the material behavior, typically at 5°C. Results from these first two steps yield the VECD model. For characterization of the viscoplastic behavior, it has been found that, in tension, constant crosshead rate tests at high temperatures, 40°C, are most appropriate (4, 21). In the outlined procedure, the VECD model is first used to predict the viscoelastic strains in the high temperature tests. These predicted strains are then subtracted from the measured strains to back-calculate the viscoplastic strains, which are then used for viscoplastic characterization.

Validation

After the development of the VEPCD model, validation tests were completed that consisted of a loading history drastically different from that used to develop the model coefficients. In this study, a random load history wherein the loading amplitude, frequency, number of cycles and sequence were randomly assigned at a temperature not used in characterization was used for this purpose. The input for the random loading validation, damage characteristic curves for each of the mixtures and the validation results are summarily presented in Figure 1. From Figure 1(c)-(f) generally good agreement between model and measurement is observed.

Additional validation tests under differing temperatures, input modes (force control or displacement control), and input levels reveal the complexity of fatigue in asphalt concrete mixtures. Results from these additional tests as well as the specifics of the given test are shown in Table 1. From this table it is observed that the mode of loading significantly influences the relative fatigue performance of the mixtures. Further, although not shown in detail here, it can be

found (21) that the fatigue ranking is not a simple function of stiffness or temperature, but rather is related in a complicated way to the resistance to deformation (stiffness), resistance to damage (C vs. S) and flow characteristics (viscoplasticity). With regard to the mode of loading dependence, it is seen from Table 1 that the performance ranking almost completely reverses with changes in the mode of loading. This finding further emphasizes the need for a comprehensive material and structural model that can accurately determine the performance of asphalt concrete pavements.

TABLE 1 Comparison of Laboratory and Field Measured Fatigue Performance

Mode of Loading	Input Amplitude	Temperature (°C)	Mixture			
			Control	CRTB	SBS	Terpolymer
Stress	Random	25	2	1	3	4
Stress	750 kPa	19	1	2	4	3
Strain	300 $\mu\epsilon$	19	4	3	2	1
Pavement Measurement		19	4	3	1	2

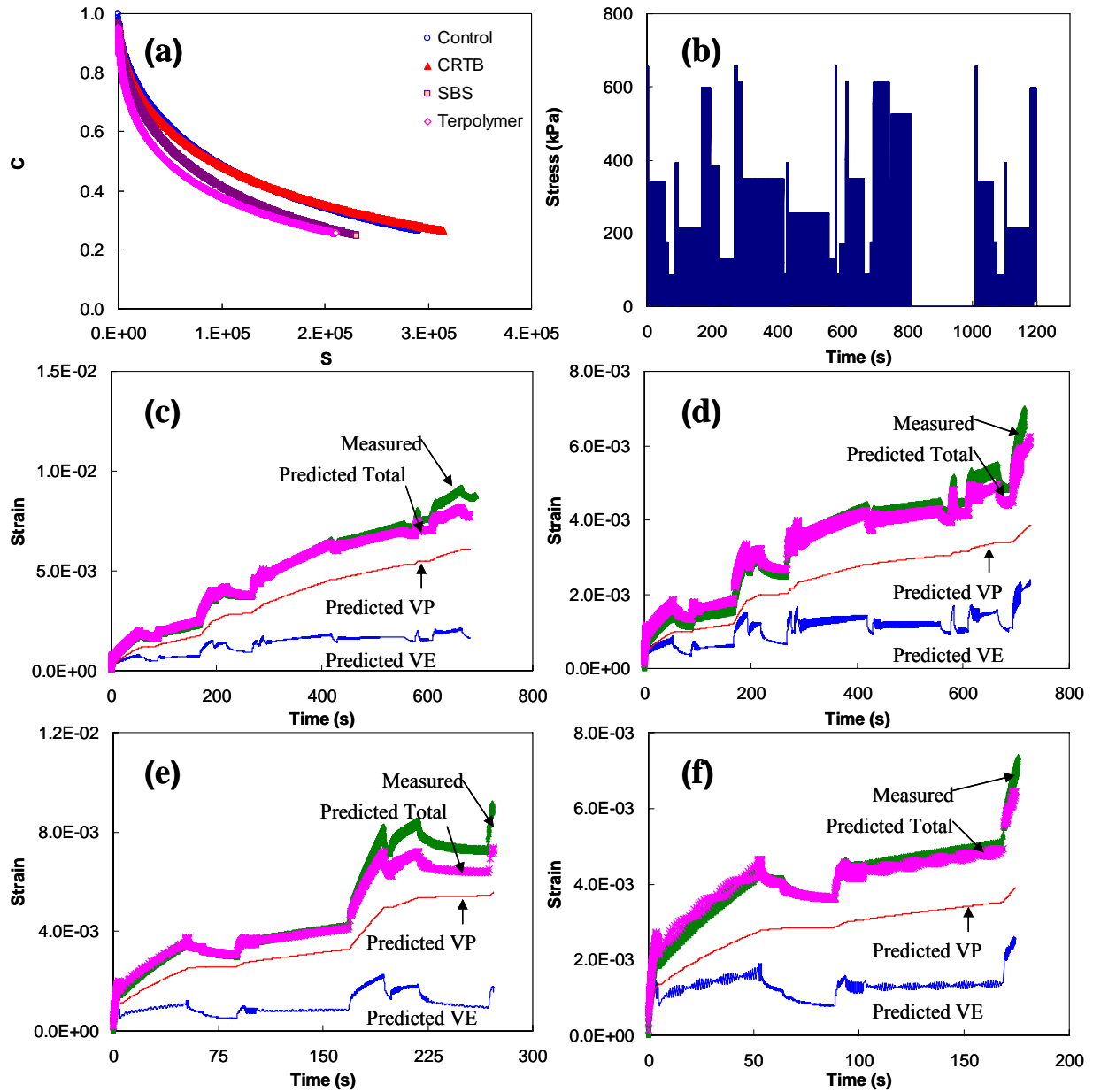


FIGURE 1 (a) Damage characteristic curves, (b) random loading input condition, random load prediction results for ALF mixtures, (c) Control, (d) CR-TB, (e) SBS, and (f) Terpolymer.

VECD-FEP++ SIMULATIONS

To gain further insight into the behavior of aggregate base asphalt concrete pavements, the VECD-FEP++ program is used to investigate the effects of asphalt layer thickness, layer stiffness, contact pressure distribution, and load level on the stresses and fatigue cracking mechanisms. Combinations of these variables are selected so that the effects of individual variables on stress and damage states can be evaluated separately and effectively. Values selected for each variable are summarized below in Table 2:

TABLE 2 Layer Thicknesses and Properties Selected in This Study

Pavement Layer	Thickness (cm) (Poisson's Ratio)	Material Parameter**			
		AC I		AC II	
Asphalt Concrete	7.6, 17.8, 30.5 (0.30)	Relaxation Time, ρ_m	Prony Coefficients, E_m (kPa)	Relaxation Time, ρ_m	Prony Coefficients, E_m (kPa)
		0.02	4908141.9	0.02	1258989.3
		0.2	5735749.4	0.2	2214693.3
		2	4955029.9	2	3621321.1
		20	2956638.2	20	5136030.7
		200	1261172.2	200	5729228.2
		2000	446992.8	2000	4459729.9
		20000	157584.1	20000	2317303.2
		E _∞ : 58269.0 kPa		E _∞ : 155243.0 kPa	
		Damage Function: $C(S) = \exp(-0.00228 \cdot S^{0.506})$			
Base	50 (0.35)	Type	k_1	k_2	k_3
		Stiff	5764.0	0.420	-0.240
		Weak	354.0	0.484	-0.403
Subgrade	Infinite (0.40)	Type	k_1	k_3	
		Stiff	474.0	-0.366	
		Weak	771.0	-0.169	
Combination		Type of Base		Type of Subgrade	
MODULUS SS		Stiff		Stiff	
MODULUS SW		Stiff		Weak	
MODULUS WS		Weak		Stiff	
MODULUS WW		Weak		Weak	
** $E(t) = E_{\infty} + \sum_{m=1}^M E_m \exp(-t / \rho_m)$ where E_{∞} , ρ_m , and E_m are infinite relaxation modulus, relaxation time, and Prony coefficients, respectively.					

An axisymmetric finite element model is employed in this study. While it is recognized that such a model will not be sufficient for the analysis of pavements with macrocracks, it is expected to be sufficient for the analysis of damage growth prior to the initiation of any macrocracks. Another important reason for this choice is the higher computational efficiency when compared with three-dimensional analysis.

Only one base thickness of 50 cm (20 in.) and infinite subgrade was selected for this study. The Prony series constants and a damage function, shown in Table 2, were obtained from the experimental study by Chehab et al. (4). The base and subgrade material parameters of the nonlinear universal model that are used are found elsewhere (11, 12).

A moving load is represented by a haversine pulse with peak magnitudes of 20 and 40 kN. A loading duration of 0.03 sec and a rest period of 0.97 sec were selected. For the tire-pavement contact pressure distribution, both uniform and nonuniform distributions were studied. The uniform contact pressure has been widely used for pavement response evaluation. However, recent studies (13-15) have revealed the nonuniformity of the contact pressure, which could lead to significant errors in actual pavement response computation. For the nonuniform tire pressure, the tire pressure measured by other researchers (16, 17) was selected for this study.

INVESTIGATION OF MACROCRACK INITIATION MECHANISMS

The research performed in this study focuses on investigating the fatigue failure mechanism(s) of top-down and bottom-up cracking modes by monitoring the state of stresses and structural damage. One unique feature of the VECD-FEP++ program is its ability to determine the amount of damage, quantified through the aforementioned damage parameter (S), in the asphalt layer as the number of loading cycles increases. Previous work indicates that major macrocracks start to develop (i.e., the point of localization) at a C of 0.3-0.2. After this point, the normal strain calculated from the displacements measured by the LVDTs is no longer meaningful, and deviations from the characteristic damage curve start to appear. This observation is important because the valid portion of the damage characteristic curve (that is, with a C value between 1 and 0.2) used in the VECD-FEP++ modeling describes various stages of cracking from the intact condition to immediately before major macrocracks develop, which leads to abrupt failure of the specimen. Therefore, it must be noted that the observations made from the VECD-FEP++ program in this paper do include the effect of initiation and propagation of microcracks. Figure 1(a) shows the relation between damage function C and damage parameter S . The damage parameter can be considered as a measure of the extent of damage and, thus, aids in the visual analysis of pavement damage preceding the development of macrocracks.

This feature of the VECD-FEP++ program is quite different from typical finite element analysis based on fracture mechanics, such as the studies done by Jenq et al. (18, 19) and Myers et al. (1). In their studies, an artificial crack was introduced before the load was applied and critical stresses that contribute most to the macrocrack propagation were identified. In this study, the approach allows the investigation of the location and mechanisms of microcracks without any initialized artificial cracks in the pavement structure.

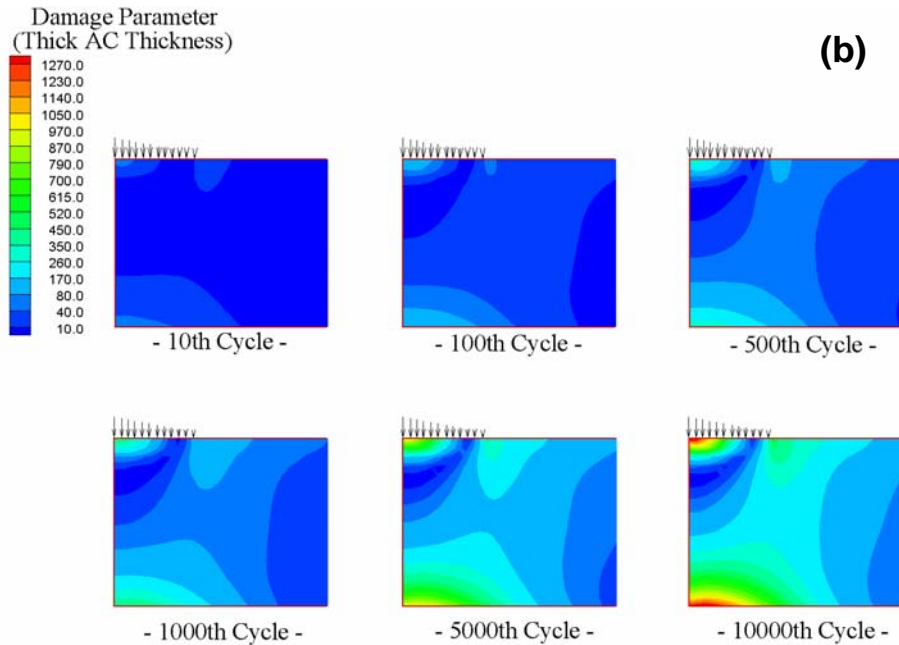
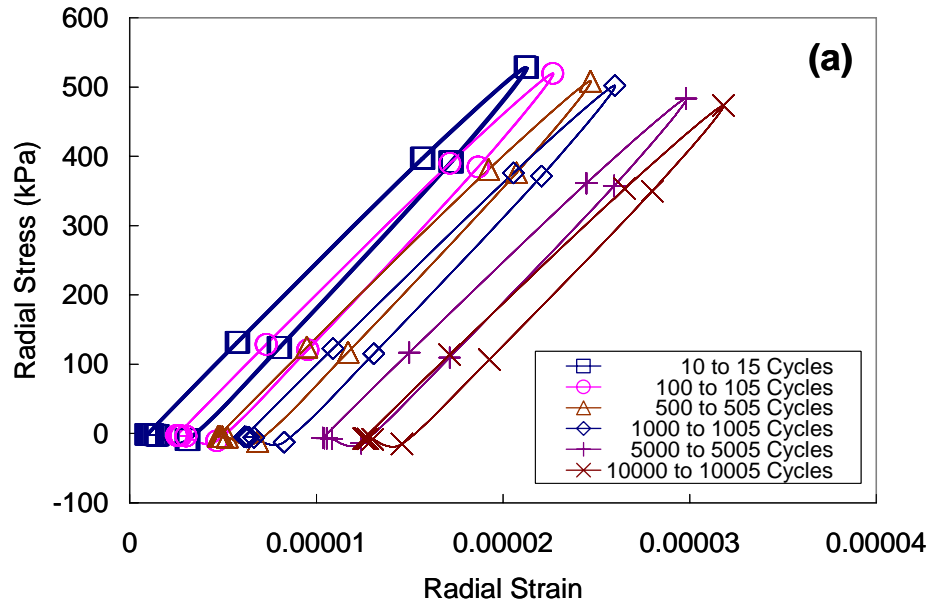


FIGURE 2 VECD-FEP++ analysis of a pavement with thick asphalt layer thickness: (a) cyclic hysteresis behavior; (b) damage contours at different cycles.

The pavement structure is modeled by an axisymmetric finite element model. Figure 2(a) shows radial stress-strain curves at the bottom of the asphalt concrete layer under nonuniform contact pressure in the cyclic mode. The hysteresis loops have shifted to the right side, demonstrating the increase of radial strain in tension as the damage in the asphalt layer increases. Figure 2(b) presents the damage contours at the various numbers of cycles. It is noted that the intensity of damage increases as the number of cycles increases.

In Figure 2(b), significant damage is found at the pavement surface near the load center where the compressive stress is the greatest. In the current formulation of the VECD-FEP++

program, the damage parameter is calculated from the absolute value of stresses. Therefore, the damage observed at the pavement surface around the load center is the damage computed from the compressive stress and, therefore, should be ignored as an error. This error is currently being corrected.

Although the VECD-FEP++ program has the ability to simulate the long-term fatigue behavior of asphalt pavements, the time required for computing becomes an issue. Simulation of the cyclic behavior of asphalt pavements using the VECD-FEP++ program takes between 5 and 7 sec/cycle on a 1.8 MHz Pentium IV computer with 512 MB memory. The simulation of 1,000 cycles takes about 1.4 to 2 hours and, based on this rate, one million cycles would take about 1,400 to 2,000 hours. To evaluate the effects of various pavement and load factors on the fatigue cracking mechanisms in an effective manner, stress distribution and damage contours at various loading cycles were examined. It was found that a comparison of stress and damage contours at the peak load of the 1,000th cycle (Figure 3 to Figure 5 and Figure 7 and Figure 8) yields similar conclusions to those made from longer cycles. For this paper, therefore, stress and damage contours at the peak load of the 1,000th cycle are used for comparison.

Figure 3 to Figure 8 show the contours of damage and stresses for all the pavement structures and loading conditions selected in this study. Figure 3 to Figure 7 were generated using the soft asphalt stiffness (i.e., AC I) only, and the effect of asphalt layer stiffness is shown in Figure 8.

In Figure 3, the following general observations can be made regarding the stresses:

1. the radial stress is in tension at the bottom of the asphalt layer and in compression at the top of the asphalt layer;
2. the shear stress is the greatest between $\frac{1}{3}$ and $\frac{1}{4}$ of the depth of the asphalt layer under the loading edge area; and
3. the axial compressive stress contour shows the largest stress in the loading center with a decreasing magnitude as the depth increases.

In the following section, a detailed evaluation of the effects of the individual variables on stress and damage states is given.

Effect of Asphalt Layer Thicknesses

Other than the general observations on the stress state listed above, two additional conclusions can be drawn from Figure 4. First, the location where the largest shear stress occurs moves from mid-depth to shallower locations as the asphalt layer thickness increases. It is noted that the maximum shear stress location is the mid-depth of the asphalt layer in the case of a thin asphalt layer thickness. For the medium and thick asphalt layer thicknesses, the maximum shear stress occurs around 7.6 to 10 cm (3 to 4 in.) below the pavement surface, regardless of the asphalt layer thickness. This observation supports findings from many field studies that the rutting in the asphalt layer, which is mainly caused by the shear flow in the mix, originates from the top 7.6 to 10 cm (3 to 4 in.) of the layer. Larger shear stresses and higher pavement temperatures during the daytime near the pavement surface may account for greater permanent deformation in this region compared to deformation in deeper locations of the layer.

Another important observation is that the level of damage is greatly affected by the asphalt layer thickness. In Figure 5, the damage value decreases significantly as the asphalt layer thickness increases. For example, the increase of the asphalt layer thickness from 7.6 to 17.8 cm (3 to 7 in.) results in a decrease in the damage level by about 60 times, as seen in the comparison between the maximum values of the contour legends, shown in Figure 5.

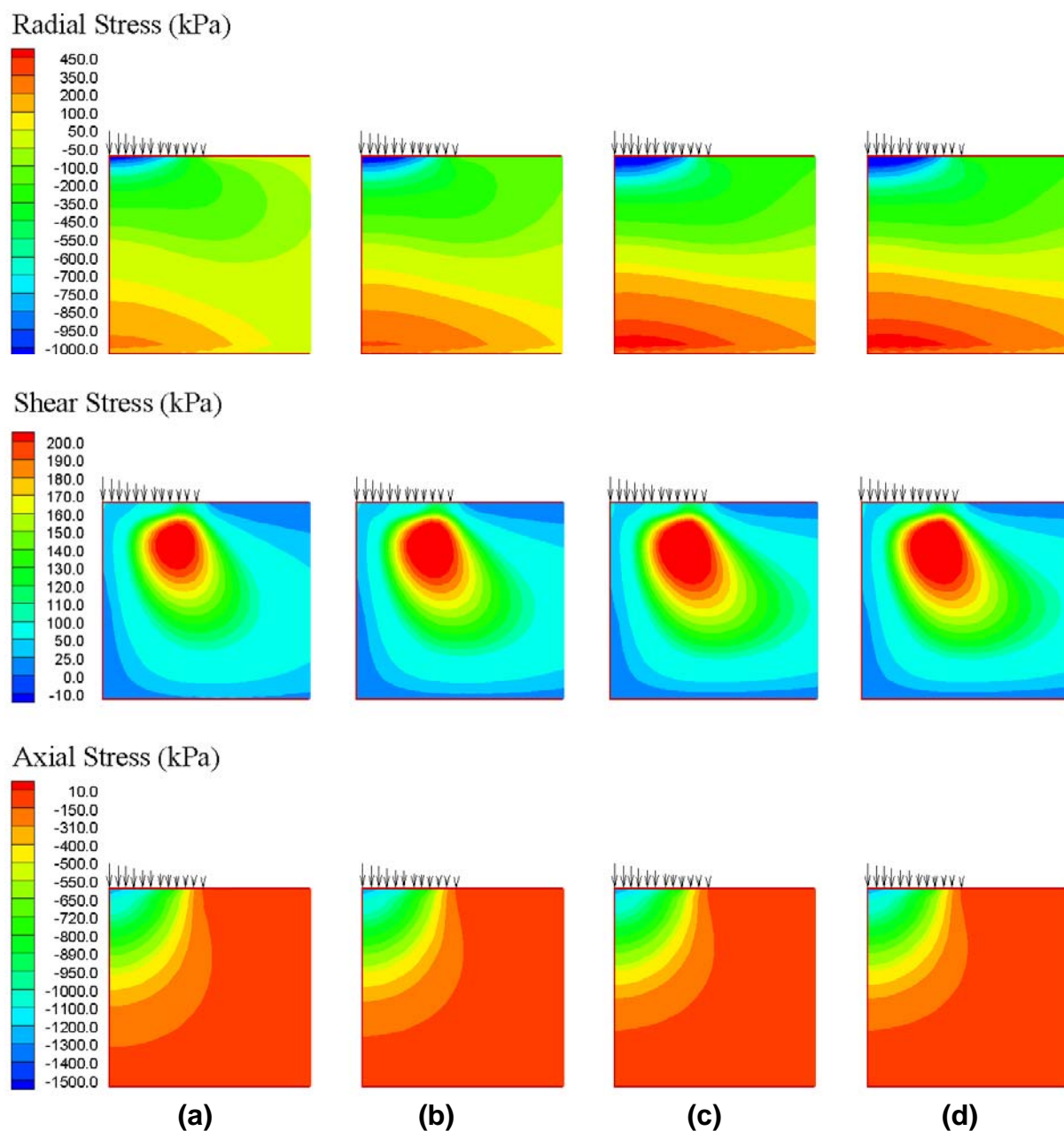
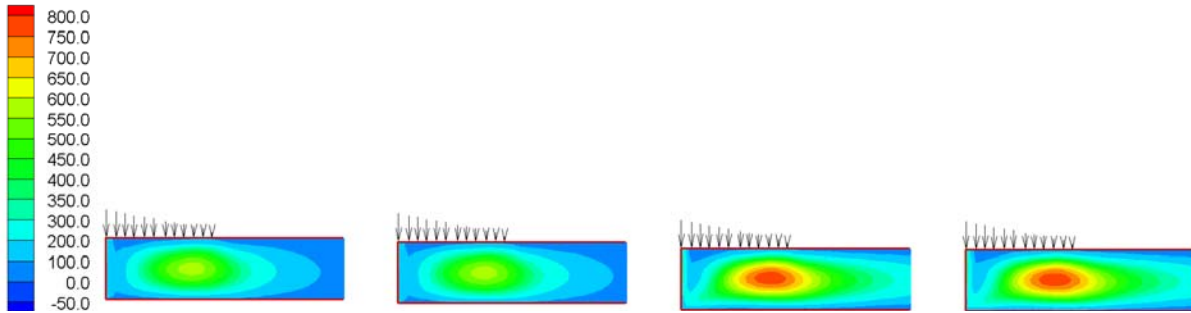
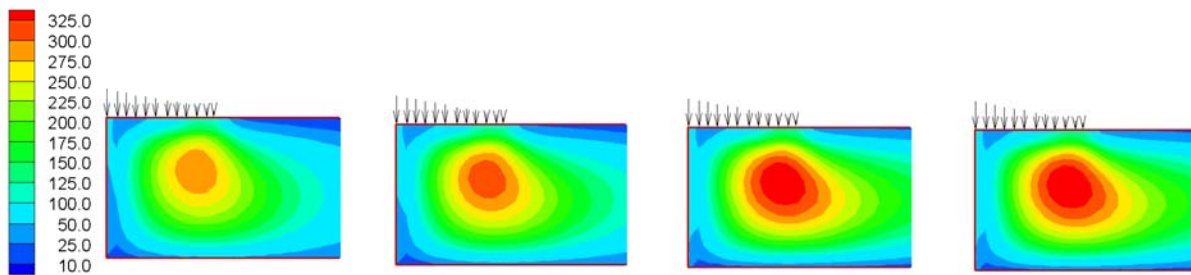


FIGURE 3 Thick asphalt layer thickness cases under nonuniform 40 kN load for: (a) MODULUS SS; (b) MODULUS SW; (c) MODULUS WS; (d) MODULUS WW (Positive stress indicates tension).

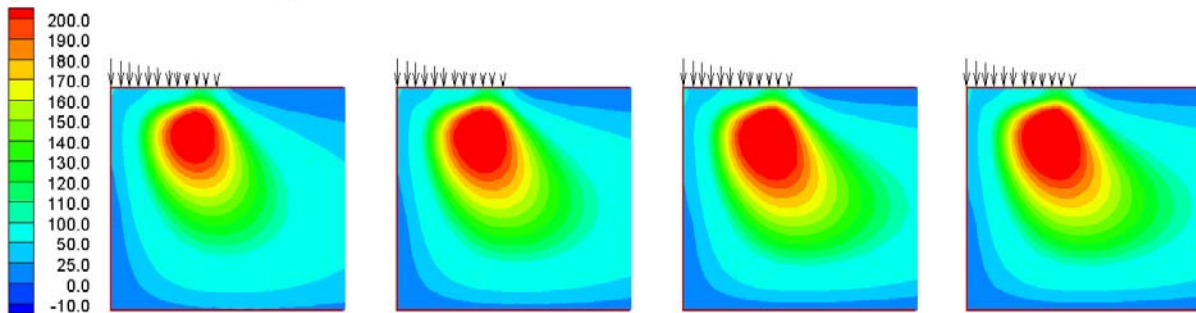
Shear Stress (kPa)
(Thin AC Thickness)



Shear Stress (kPa)
(Medium AC Thickness)



Shear Stress (kPa)
(Thick AC Thickness)



(a)

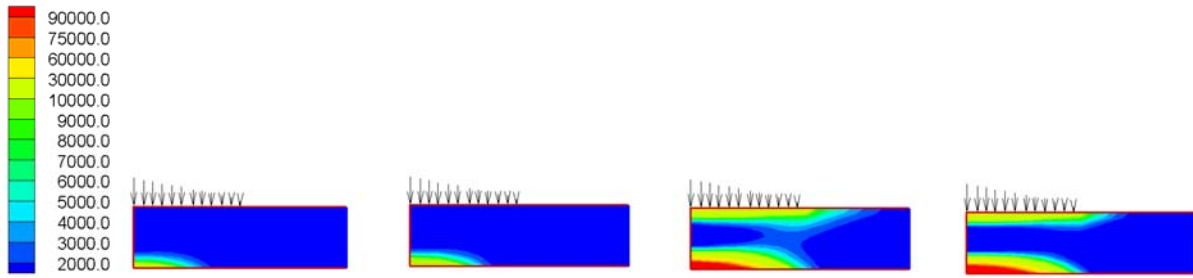
(b)

(c)

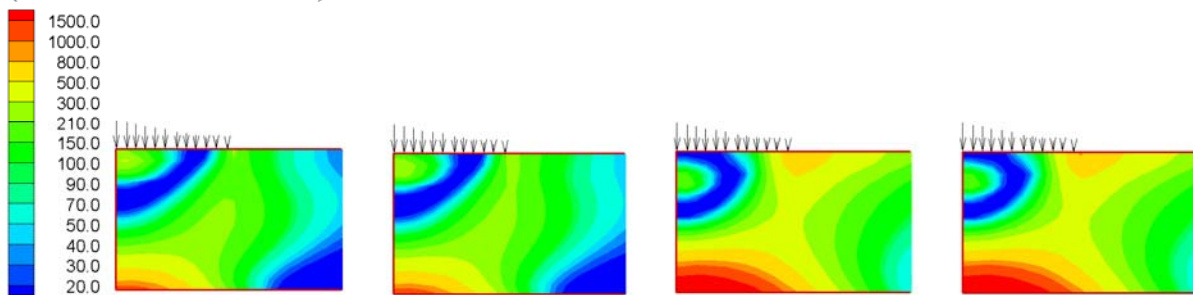
(d)

FIGURE 4 Shear stresses in the asphalt layer under nonuniform 40 kN load for: (a) MODULUS SS; (b) MODULUS SW; (c) MODULUS WS; (d) MODULUS WW.

Damage Parameter
(Thin AC Thickness)



Damage Parameter
(Medium AC Thickness)



Damage Parameter
(Thick AC Thickness)

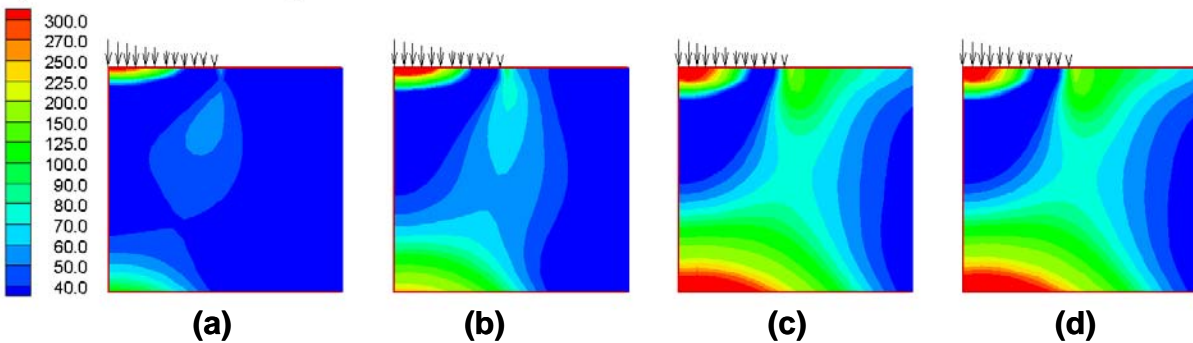


FIGURE 5 Damage contours in varying asphalt layer thicknesses under nonuniform 40 kN load for: (a) MODULUS SS; (b) MODULUS SW; (c) MODULUS WS; (d) MODULUS WW.

Finally, the most important observation from Figure 5 is the change in the location of crack initiation as a function of the asphalt layer thickness. When the thinnest layer is modeled in Figure 5, the severe damage is found at the bottom of the layer with negligible damage at the top of the asphalt layer. As the asphalt layer becomes thicker, damage directly under the tire edge starts to emerge, in addition to that at the bottom of the asphalt layer. In the thickest asphalt layer case, the intensity of damage under the tire edge is as high as that at the bottom of the asphalt layer.

The different cracking mechanisms between thin and thick asphalt layers can be seen more effectively when Figure 2(b) and Figure 6 are compared. In the thin layer, shown in Figure 6, the damage evolution is governed mostly by the damage that started from the bottom of the asphalt layer. However, in the thick asphalt layer, shown in Figure 2(b), damage initiates from both the bottom of the asphalt layer and at the tire edge, and propagates simultaneously to form a conjoined damage contour. This conjoined damage contour, shown in Figure 2(b) and Figure 5 for the medium and thick asphalt pavements, supports the findings from field studies of top-down cracking (20); that is, the top-down cracks are found in asphalt pavements with an asphalt layer thicker than 25 to 30 cm (10 to 12 in.).

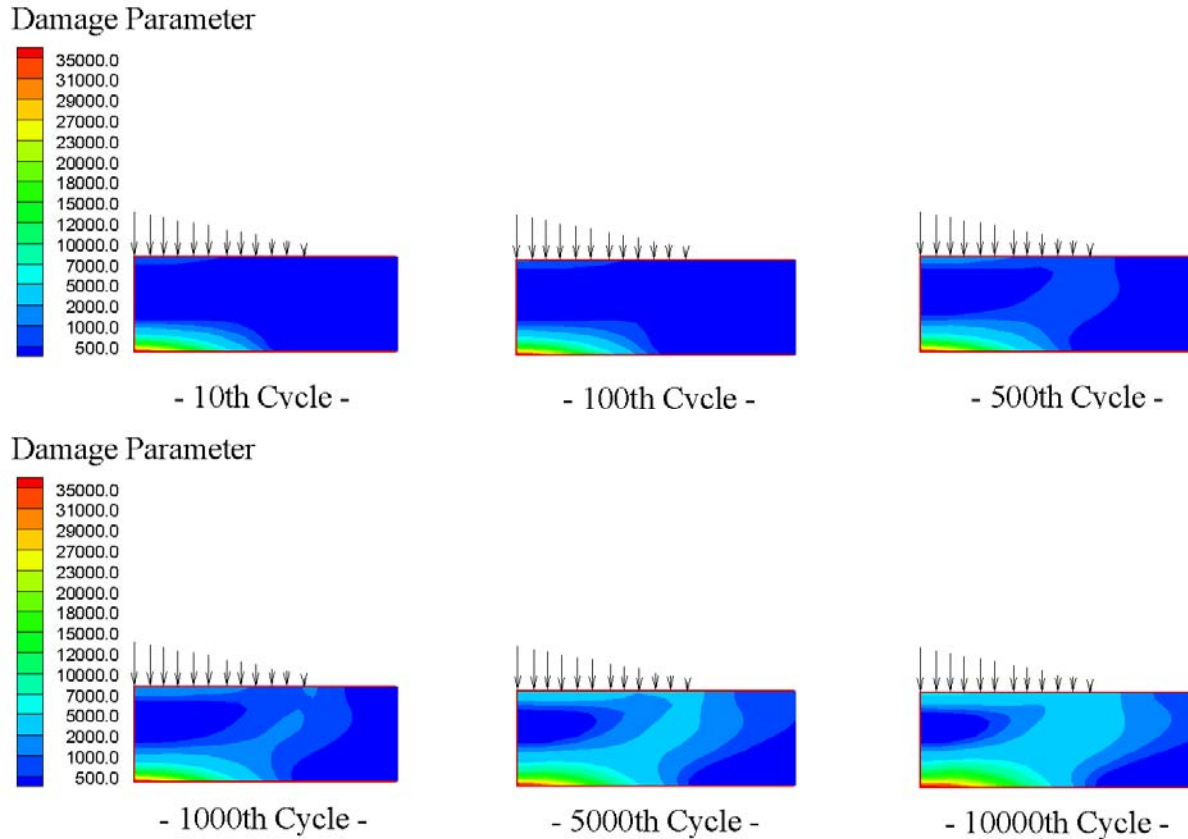
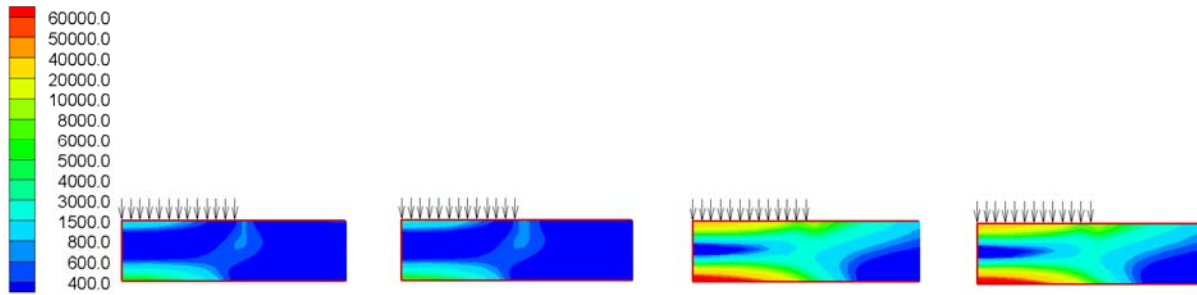
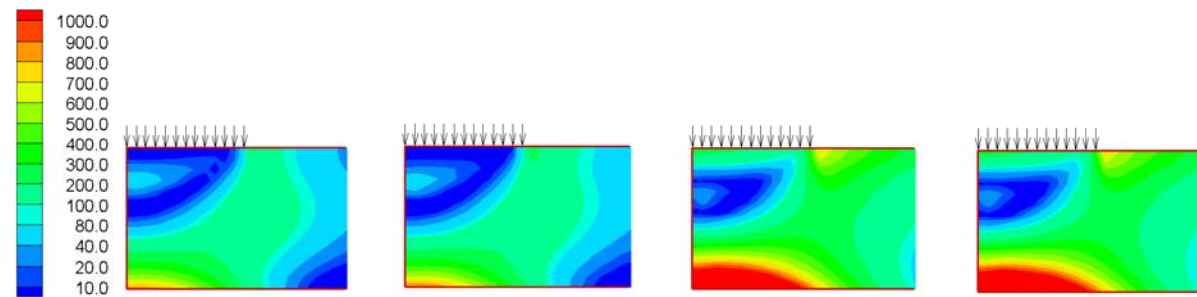


FIGURE 6 Damage evolution in the thin asphalt layer.

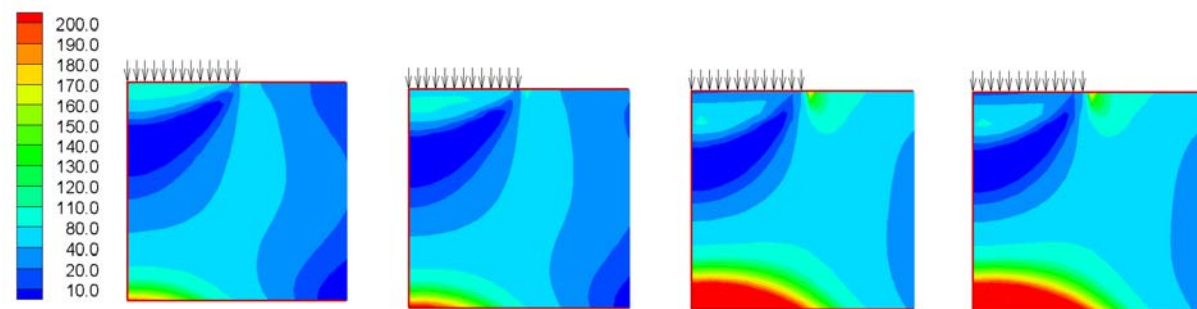
Damage Parameter
(Thin AC Thickness)



Damage Parameter
(Medium AC Thickness)



Damage Parameter
(Thick AC Thickness)



(a)

(b)

(c)

(d)

FIGURE 7 Damage contours in varying asphalt layer thicknesses under uniform 40 kN load for: (a) MODULUS SS; (b) MODULUS SW; (c) MODULUS WS; (d) MODULUS WW.

Also, the conjoined damage contour suggests that the through-the-thickness crack may develop as these bottom-up and top-down microcracks propagate further and coalesce together. Gerritsen et al. (20) reported the finding of single field cores with top-down cracking for about 10 cm (4 in.), no cracking at all for about 5 cm (2 in.), and bottom-up cracking for about 10 cm (4 in.). The conjoined damage contour in Figure 2(b) and Figure 5 explains the reason behind this observation. This finding clearly demonstrates the problem associated with the traditional approach to fatigue performance prediction where the tensile strain at the bottom of the asphalt layer is related to the fatigue life of the pavement. This approach cannot account for the

additional crack growth from the top of the pavement and, therefore, overestimates the fatigue life of the pavement.

Effect of Contact Pressure Distributions

The issue of contact pressure distribution has been discussed previously. Figure 5 and Figure 7 show the results from the nonuniform and uniform contact pressures, respectively. One observation that can be made from the comparison of the figures is that the nonuniform pressure distribution results in a greater amount of damage in all the cases. For example, Figure 5, with the nonuniform contact pressure, shows greater damage than Figure 7 with the uniform contact pressure when the values of the contour legends are compared. This difference suggests that the pavement responses, calculated in the traditional way of treating the tire pressure as uniform, may underestimate the actual damage in the field and thereby overestimate the pavement service life. Also, it needs to be noted that the propensity of top-down cracking becomes greater under nonuniform pressure than under uniform pressure. This observation supports findings from laboratory tests conducted by Groenendijk et al. (14) and Miradi et al. (15) who showed that a nonuniform load causes large stresses at the pavement surface.

Effect of Base and Subgrade Moduli

The effect of base and subgrade moduli can be evaluated by comparing four subfigures under each response parameter in each figure. First of all, Figure 5 and Figure 7 indicate that the effect of the subgrade modulus on damage states is much less than the effect of the base modulus. Regarding the crack initiation location, the weaker base and/or weaker subgrade increases the intensity of damage under the tire edge and, therefore, the propensity of top-down cracking. In the thickest asphalt layer, the weaker base results in more damage in general, but this trend is more evident in the damage under the tire edge.

Effect of Asphalt Layer Stiffness

Figure 8 presents the damage contours calculated using two asphalt layer stiffnesses (AC I and AC II in Table 2) under both nonuniform and uniform pressure distributions. It can be concluded from this figure that the damage under the tire edge becomes slightly greater as the stiffness of the asphalt layer increases. This observation may become important when the aging of the asphalt layer is considered. It is known that aging is more severe at the top portion of the asphalt layer. The stiffening effect of aging, therefore, makes the top portion of the asphalt layer stiffer than the rest of the layer, which in turn increases the tendency of top-down cracking.

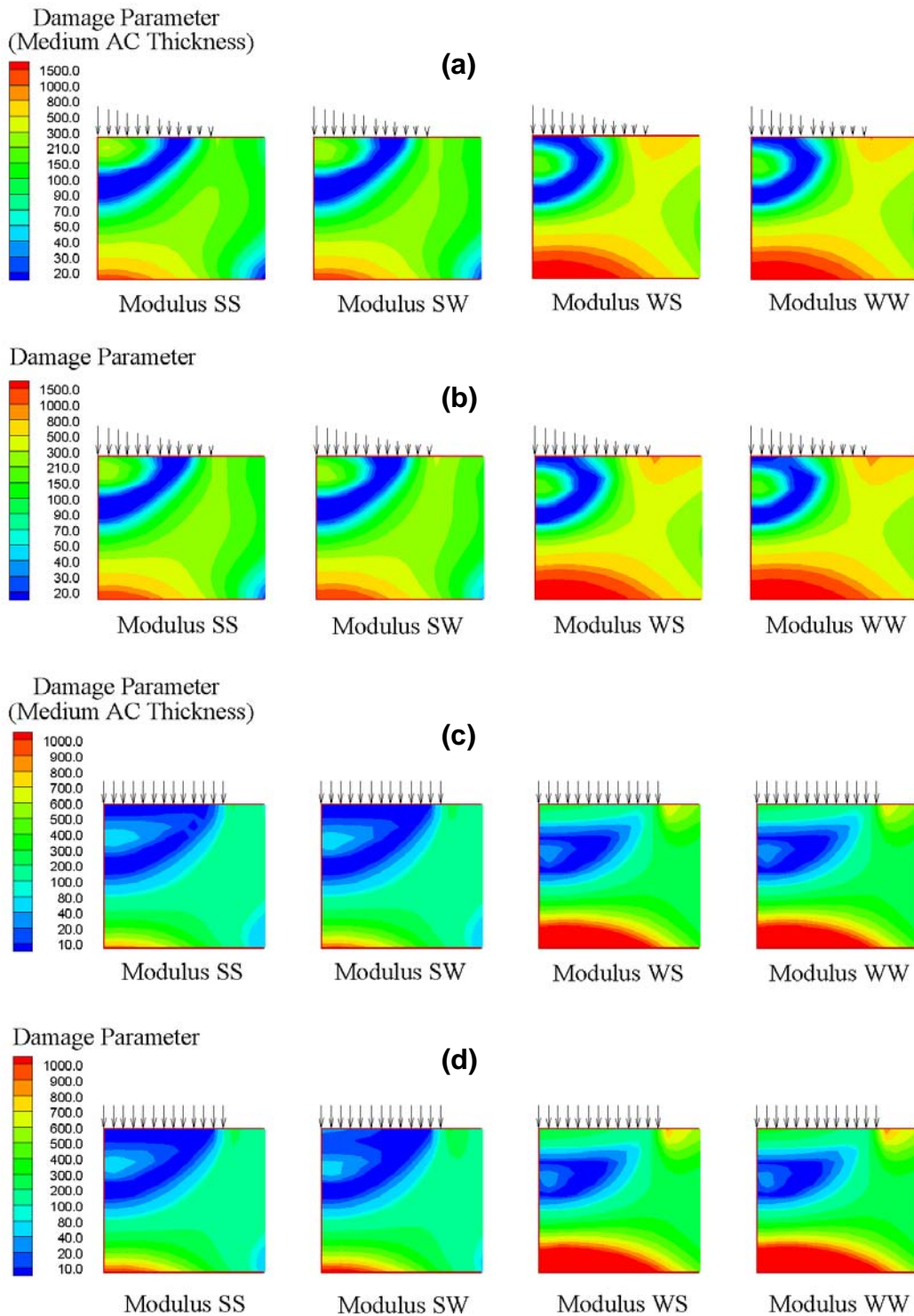


FIGURE 8 Damage contours in the medium thick asphalt layer: (a) nonuniform pressure and AC stiffness; (b) nonuniform pressure and AC II stiffness; (c) uniform pressure and AC I stiffness; (d) uniform pressure and AC II stiffness.

CONCLUSIONS

It is demonstrated that the VECD-FEP++ program, with a damage characteristic curve determined from a single monotonic test and the time-temperature shift factor determined from the complex modulus test, may be used to study the cracking mechanisms of asphalt pavements. The findings from this study show the effect of various pavement and load factors on pavement responses as well as damage in the asphalt layer. The most important conclusions from this parametric study can be summarized as follows:

1. The asphalt layer thickness has a significant effect on the magnitude and location of damage.
2. The damage contour is affected more by the base stiffness than by the subgrade and asphalt layer stiffnesses.
3. Nonuniform pressure causes larger stresses and greater damage than uniform pressure.
4. The propensity of top-down cracking increases as: (1) the asphalt layer becomes thicker; (2) the contact pressure becomes nonuniform; (3) the base and/or subgrade become less stiff; and (4) the asphalt layer becomes stiffer.
5. The conjoined damage contours in thicker pavements suggest that the through-the-thickness crack may develop as these bottom-up and top-down cracks propagate simultaneously and coalesce together. This observation raises a serious question as to the validity of the traditional fatigue performance prediction approach in which only the tensile strain at the bottom of the asphalt layer is considered in predicting the fatigue life of asphalt pavements.
6. The damage level computed by the VECD-FEP++ program provides a direct way of determining the Equivalent Axle Load Factor of different load levels.

ACKNOWLEDGMENTS

The authors would like to acknowledge the financial support provided by the Federal Highway Administration.

REFERENCES

1. Myers, L. A., R. Roque, and B. Birgisson. Propagation Mechanisms for Surface-initiated Longitudinal Wheel Path Cracks. *Transportation Research Record 1778*, TRB, National Research Council, Washington, D.C., 2001, pp. 113-122.
2. Kim, Y. R., H. J. Lee, and D. N. Little. Fatigue Characterization of Asphalt Concrete Using Viscoelasticity and Continuum Damage Theory. *Journal of the Association of Asphalt Paving Technologists*, Vol. 66, 1997, pp. 520-569.
3. Daniel, J. S. and Y. R. Kim. Development of a Simplified Fatigue Test and Analysis Procedure Using a Viscoelastic Continuum Damage Model. *Journal of Association of Asphalt Paving Technologists*, 2002, Vol. 71, pp. 619-650.
4. Chehab, G. R., Y. R. Kim, R. A. Schapery, M. W. Witzak, R. Bonaquist. Time-Temperature Superposition Principle for Asphalt Concrete Mixtures with Growing Damage in Tension. *Journal of Association of Asphalt Paving Technologists*, 2002, Vol. 71, pp. 559-593.
5. Guddati, M. N. *FEP++: A Finite Element Program in C++*. Input Manual, Department of Civil Engineering, North Carolina State University, 2001.
6. Mun, S. *Nonlinear Finite Element Analysis of Pavements and Its Application to Performance Evaluation*. Ph.D. Dissertation, Department of Civil Engineering, North Carolina State University, 2003.

7. Witczak M. W. and J. Uzan. *Universal Airport Pavement Design System, Report I of IV: Granular Material Characterization*. Department of Civil Engineering, University of Maryland, College Park, 1988.
8. Raad, L. and J. L. Figueroa. Load Response of Transportation Support Systems. *Transportation Engineer Journal*, Vol. 106, No. 1, 1980, pp. 111-128.
9. Harichandran, R. S., G. Y. Baladi, and M. S. Yeh. *Development of a Computer Program for Design of Pavement Systems Consisting of Bound and Unbound Materials*. Department of Civil and Environmental Engineering, Michigan State University, 1989.
10. Hjelmstad, K. D. and E. Taciroglu. Analysis and Implementation of Resilient Modulus Models for Granular Solids. *Journal of Engineering Mechanics*, Vol. 126, No. 8, ASCE, 2000, pp. 821-830.
11. Santha, B. L. Resilient Modulus of Subgrade Soils: Comparison of Two Constitutive Equations. *Transportation Research Board 1462*, TRB, National Research Council, Washington D.C., 1994, pp. 79-90.
12. Garg, N. and M. R. Thompson. *Mechanistic-Empirical Evaluation of the Mn/ROAD Low Volume Road Test Sections*. Illinois Cooperative Highway and Transportation Research Program Report FHWA-IL-UI-262, Urbana, IL, 1998.
13. Sebaaly, P. E. and N. Tabatabaee. Influence of Vehicle Speed on Dynamic Loads and Pavement Response. *Transportation Research Board 1410*, TRB, National Research Council, Washington D.C., 1993, pp. 107-114.
14. Groenendijk, J., C. H. Vogelzang, A. A. A. Molenaar, B. R. Mante, and L. J. M. Dohmen. Linear Tracking Response Measurements: Determining Effects of Wheel-Load Configurations. *Transportation Research Record 1570*, TRB, National Research Council, Washington, D.C., 1997, pp. 1-9.
15. Miradi, A., J. Groenendijk, and L. J. M. Dohmen. Crack Development in Linear Tracking Test Pavements from Visual Survey to Pixel Analysis. *Transportation Research Record 1570*, TRB, National Research Council, Washington, D.C., 1997, pp. 48-54.
16. Sebaaly, P. E. *Dynamic Forces on Pavements: Summary of Tire Testing Data*. Report on FHWA Project DTFH 61-90-C-00084, 1992.
17. Siddharthan, R. V., N. Krishnamenon, M. El-Mously, and P. E. Sebaaly. Investigation of Tire Contact Stress Distributions on Pavement Response. *Journal of Transportation Engineering*, Vol. 128, No. 2, ASCE, 2002, pp. 136-144.
18. Jenq, Y-S. and J-D. Perng. Analysis of Crack Propagation in Asphalt Concrete Using Cohesive Crack Model. *Transportation Research Record 1317*, TRB, National Research Council, Washington, D.C., 1991, pp. 90-99.
19. Jenq, Y-S., C-J. Liaw, and P. Liu. Analysis of Crack Resistance of Asphalt Concrete Overlays - A Fracture Mechanics Approach. *Transportation Research Record 1388*, TRB, National Research Council, Washington, D.C., 1993, pp. 160-166.
20. Gerritsen, A. H., C. A. P. M. Van Gorp, J. P. J. Van der Heide, A. A. A. Molenaar, and A. C. Pronk. Prediction and Prevention of Surface Cracking in Asphalt Pavements. 6th *International Conference on Structural Design and Asphalt Pavements*, The University of Michigan, Ann Arbor, Michigan, 1987, pp. 378-391.
21. Underwood, B. S., Y. R. Kim and M. N. Guddati. Characterization and Performance Prediction of ALF Mixtures Using a Viscoelastoplastic Continuum Damage Model. *Journal of Association of Asphalt Paving Technologists*, 2006, Vol. 75.

22. Schapery, R. A. Nonlinear Viscoelastic and Viscoplastic Constitutive Equations with Growing Damage. *Int. Journal of Fracture*, Vol. 97, pp. 33-66.
23. Uzan, J. Asphalt Concrete Characterization for Pavement Performance Prediction. *Journal of Association of Asphalt Paving Technologists*. Vol. 65, pp.573-607.